2011 International Nuclear Atlantic Conference - INAC 2011
Belo Horizonte,MG, Brazil, October 24-28, 2011
ASSOCIAÇÃO BRASILEIRA DE ENERGIA NUCLEAR - ABEN
ISBN: **978-85-99141-04-5**

HYDROSTATIC PRESSURE CELLS DEVELOPMENT FOR X-RAY AND NEUTRONS EXPERIMENTS

José Luís Passamai Jr[1], Christiano J.G. Pinheiro[1], Marcos Tadeu D. Orlando[1], Hamilton P.S. Correa[2], Jesualdo L. Rossi[3], Vera L. Mazzocchi[3], Carlos B.R. Parente[3], José M. Filho[3], Francisco C.L. de Melo[4], Luis G. Martinez[3] and Carlos A.C.Passos[1]

[1] Departamento de Física
Universidade Federal do Espírito Santo
Avenida Fernando Ferrari, 514
29075-910 Vitória, ES
christrieste@yahoo.it

[2] Universidade Federal do Mato Grosso do Sul
Cidade Universitária
79070-900 Campo Grande, MS
hpsoares@gmail.com

[3] Instituto de Pesquisas Energéticas e Nucleares (IPEN / CNEN - SP)
Av. Professor Lineu Prestes 2242
05508-000 São Paulo, SP
jelrossi@ipen.br

[4] Departamento de Ciência e Tecnologia Aeroespacial
Centro Tecnológico da Aeronáutica – CTA
Avenida Brigadeiro Faria Lima, 1941
12227-000 São José dos Campos, SP
frapi@iae.cta.br

ABSTRACT

A set of hydrostatic pressure cells was specially developed in order to be applied in X-ray diffraction, X-ray absorption and neutron diffraction experiments. For the experiments where X-rays are used, the pressure cells are built in a CuBe alloy body with two B_4C anvils in order to allow the low absorption of the radiation. The B_4C anvils were specially prepared in CTA - Centro Técnico Aeroespacial - São José dos Campos - Brazil, in order to present enhanced X-ray transparency and high hardness. One of the advantage of the CuBe-body cell with B_4C anvil is that it can be also used under magnetic fields, for instance for measurements of AC magnetic susceptibility under high hydrostatic pressures. The X-ray cells work in transmission mode and present a 2mm diameter hole for the beam path. The X-ray beam pass through the hole and outgoing to the detector positioned in front of the pressure cell. A second type of pressure cell was developed in order to be used in neutron elastic scattering experiments, especially in neutron diffraction experiments. The neutron cell pressure cell was constructed in Zirconium alloy reinforced with carbon fibers composite in order to improve the mechanical resistance of his cylindrical geometry. The B_4C pressure cells are available to users of the techniques of X-ray diffraction and absorption in the Brazilian National Synchrotron Laboratory – LNLS, at Campinas City. The neutron pressure cell is available to users at the neutron powder diffraction facility installed at the Nuclear and Energy Research Institute – IPEN, São Paulo. In this work will be shown details and drawings of the two types of hydrostatic pressure cells.

1. INTRODUCTION

Ordered double perovskite oxides, whose general formula is $A_2B'B''O_6$, were first proposed by Longo and Ward [1] in 1961. According to those authors, *A* is an alkaline-earth divalent cation, *B*' and *B*'' are transition-metals and present an octahedral coordination with the anion O^{-2} [2]. This type of compound exhibits magnetic and electronic properties related to the strong interplay between structure, charge and spin ordering [3], which is the subject of nano-spintronic studies. Spintronics is an emerging field of science and technology that will most likely have a significant impact on the future of all aspects of electronics [4-6]. Moreover, spintronics is the next step towards the new technology of spin-based quantum computing and quantum information processing [7-9], voltage controlled spintronic devices for logical applications [10] and semiconductor devices [11,12].

The early discovery of large low-field room-temperature magnetoresistance in these compounds (mainly in half-metallic Sr_2FeMoO_6, described by Kobayashi in 1998 [13]) stimulated interest in the study of the properties of ordered double perovskites, in the context of their potential application in the field of spin electronics [14-17]. The focus of these studies was to characterize their magnetic and electronic properties as well as their crystallographic structures. Among them, the A_2MReO_6 series (namely Re-based ordered double perovskites), with *A* = Ba, Sr, Ca and *M* = Cr, Fe, Mn, shows a wide variety of magnetic and electronic properties. Concerning the magnetic state, the majority of the compounds reveal ferromagnetic behavior with the coupling of the divalent magnetic *M* ion to Re [18].

The ideal structure of the double perovskites is based on the adapted tolerance factor *t* of the single perovskite [19]. In general, for double perovskites $A_2B'B''O_6$, the tolerance factor can be written as

$$t = \frac{r_A + r_O}{\sqrt{2}\left(\frac{r_{B'}}{2} + \frac{r_{B''}}{2} + r_O\right)} \quad (1)$$

where r_A, r_B and $r_{B''}$ are the ionic radii of the respective ions and r_O is the ionic radius of oxygen. The closer to $t = 1$, the more the structure corresponds to ideal cubic. Therefore, except in rare cases, one can consider the following rule for the double perovskite family: for $1.05 > t > 1.00$ a cubic structure is adopted within the $Fm\bar{3}m$ space group; for $1.00 > t > 0.97$ the most likely structure corresponds to the $I4/m$ tetragonal space group and if $t < 0.97$ the compound becomes either monoclinic ($P2_1/n$) or orthorombic [20]. Philipp *et al.* [18] reached a similar conclusion by studying the CrW-based series. Lufaso *et al.* [19] reported that roughly 70% of all ordered double perovskites undergo octahedral tilting distortions. By considering 11 possible distinct types of octahedral tilting, it was shown that five tilted systems accounted for ~97% of the reported structures. The five dominant tilted systems reported, namely $Fm\bar{3}m$ ($a^0a^0a^0$), $I4/m$ ($a^0a^0c^-$), $R\bar{3}$ ($a^-a^-a^-$), $I2/m$ ($a^0b^-b^-$) and $P2_1/n$ ($a^-a^-b^+$), as well as two additional tilted systems, $Pn\bar{3}$ ($a^+a^+a^+$) and $P4/mnc$ ($a^0a^0c^+$), can be simulated using the *SPuDS* (Structure Prediction Diagnostic Software) [21].
Several reports like the ones by Philipp *et al.* [16] and Popov *et al.* [22] have studied the correlation between the *A*-site cation size and the properties of the double perovskites. Granado *et al.* [23] have concentrated on the spin-orbital manifestation of Re ion and its

influence on the electronic properties of the Ca_2FeReO_6 compound. Herrero-Martín *et al.* [24] studied the X-ray absorption of the FeRe-base double perovskites series employing the most recent theoretical calculations in order to explain the magnetic and electronic results. Sikora et al. [25], employing X-ray magnetic circular dichroism at the Re $L_{2,3}$ edges, observed a considerable orbital magnetic moment, which implies an unquenched Re orbital moment, despite its octahedral coordination [26], in the similar series of FeRe-based double perovskites made by Herrero-Martín [24]. Finally, Serrate et al. [20] published a large topical review showing the importance of these materials for spintronic devices and that the physics involved in these compounds is more complex and rich than expected.

This work was proposed by taking into account a scenario which the magnetic and electronics properties of the Ca_2MnReO_6 double perovskite present a strong correlation with structural order. The main goal was to investigate pressure cell performance observing the behavior of ReO_6 under pressure. The knowledge of ReO_2 octahedral under pressure will be applied as an important tool to understand its correlation with and crystal structure of the monophasic compound Ca_2MnReO_6.

2. EXPERIMENTAL AND RESULTS

2.1. Cell Pressure

The B_4C anvil pressure cell described here was designed and built for use in XAS and angle-dispersive X-ray scattering experiments under hydrostatic pressures up to 1.2 GPa. The first advantage of the B_4C anvil pressure cell is that anvils of sintered B_4C yield an X-ray absorption spectrum free of Bragg peaks, in contrast to spectra taken through diamond anvils. The second advantage over conventional diamond anvil cells (DACs) is the large transmission coefficient of incoming X-rays (>60% at 10 keV) and the applicability of the B_4C cell in experiments that require lower pressure (up to 1.0 GPa) compared with the conventional DAC pressure range. The third advantage is the relatively low costs (approximately half the price of a DAC) for development and manufacture. The fourth and main advantage of this home-built B_4C anvil pressure cell is that the body of the cell is made of CuBe alloy to allow magnetic measurements without interference. Using this concept it was possible to measure AC magnetic susceptibility, X-ray absorption and diffraction using synchrotron radiation with the same pressure cell. The anvils were made of B_4C powder supplied by Hermamann C. Stark, Inc. (Berlin, Germany) with a specific area of 7.9 kg m^{-2} and pyrolitic carbon as sintering additive.

To improve the transmitted X-ray intensity, the thickness at the center of the anvil was reduced as follows. A hole of diameter 2 x 10^{-3} m and depth 3 x 10^{-3} m was made on one side of each B_4C anvil using a diamond drill. The anvil was mounted in a CuBe cavity forming a block, which was used to press the gasket. Its angular exit aperture is approximately 30º 2θ. The figure 1 shows a schematic drawing of the B_4C anvil pressure cell with the following details: (a) non-magnetic CuBe cell body, (b) B_4C anvil, (c) external coil (AC magnetic field generator), (d) CuBe gasket and (e) pickup coil. In both B_4C anvils the largest (smallest) diameter is 8 x 10^{-3}m (4 x 10^{-3} m). The gasket set-up for X-ray absorption fine structure (XAFS) measurements had ReO_3 and α-ReO_2 inside the hole, while the set-up for diffraction had only α -ReO_2. In both cases there was an O-ring made of $Hg_{0.8}Re_{0.2}Ba_2Ca_2Cu_3O_{8.8}$ (Hg, Re-1223) superconductor around the gasket hole wall.

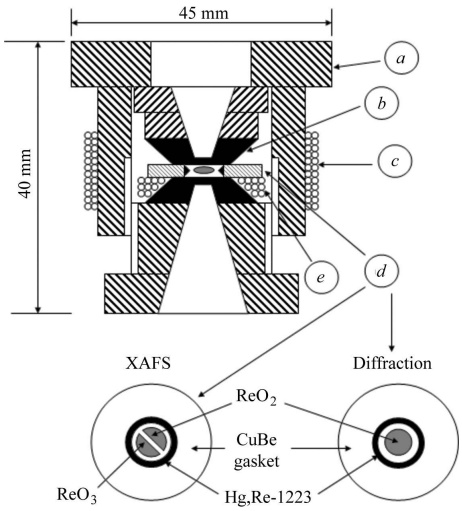

Figure 1 - Schematic drawing of the pressure cell and gaskets.

Hydrostatic pressure conditions were obtained by filling the CuBe gasket hole (2 x 10^{-3} m in diameter and 0.45 x 10^{-3} m thick) with a mineral oil/n-pentanol mixture (1/1). The inner pressure was calibrated using a superconducting $Hg_{0.8}Re_{0.2}Ba_2Ca_2Cu_3O_{8.8}$ (Hg,Re-1223) manometer placed in the gasket cavity and mounted in the inner gasket border, forming a ring outside the X-ray beam spot (Fig. 1).

2.2 Conventional XAS

The local ReO_6 octahedral oxygen coordination was investigated by extended X-ray absorption fine structure (EXAFS) using the D04B-XAFS1 beamline [26] for cubic ReO_3 (ICDD card #03-065-7483) and monoclinic α-ReO_2 powdered samples. Ex situ measurements were recorded three times at the Re L_{III}-edge (10.535 keV) in transmission mode at room temperature and averaged. The monochromator was a channel-cut Si(111) (2d = 6.271 Å) crystal. Energy calibration was carried out using the first inflection point of the XANES spectrum of Pt (L_{III}-edge 11.564 keV), Zn (K-edge 9.659 keV) and Ta (L_{III}-edge 9.881 keV) foils as references.

2.3 EXAFS under pressure.

To verify the pressure performance of the B_4C cell, the first compound investigated under external hydrostatic pressure was Ca_2MnReO_6 powder. The ReO_6 octahedral present in this double perovskite is a pressure sensitive system owing to its second-order transition (compressibility collapse), which occurs at approximately 0.5 GPa [27]. This behavior is similar to the structure of ReO_3, which is Pm3m up to 0.5 GPa [28], and above this pressure it transforms to Im3, which is stable up to 2.8 GPa. Compression of the low-pressure Pm_33m phase occurs via compression of Re—O bonds [28]. However the Re—O—Re bond angle changes at pressures between 0.6 and 2.8 GPa, as observed by [29] in XAS and neutron diffraction measurements.

XAS measurements of Ca_2MnReO_6 at ambient pressure and 0.6 and 1.2 GPa were carried out at the D04B-XAS beamline. To improve the image quality the figure 2 shows the FFT of the EXAFS spectra for ambient pressure, 0.6 and 1.2 GPa. The FFT of the pressure-dependent Ca_2MnReO_6 dispersive EXAFS spectra times k^2 [$\chi(k)k^2$] performed at the Re LIII-edge (10.535 keV). The full line is the output fit from FEFFIT8 times k^2 after FFT, using a range $0.2 < k < 10.5$ Å^{-1}. The accumulation time for each dispersive XAFS spectrum was 650 ms, and the final spectrum was taken as an average over 50 accumulations. The beam was focused to a spot of size $0.3x10^{-3}$ m x $0.3x10^{-3}$ m in the center of the O-ring made of (Hg,Re-1223) superconductor (inner pressure gauge) in which the α-ReO_2 and ReO_3 were mounted. The I_0 (intensity without sample) reference spectrum was obtained using an identical (but empty) pressure cell mounted beside the first one. For each pressure value the I_0 spectrum was taken at the same time interval.

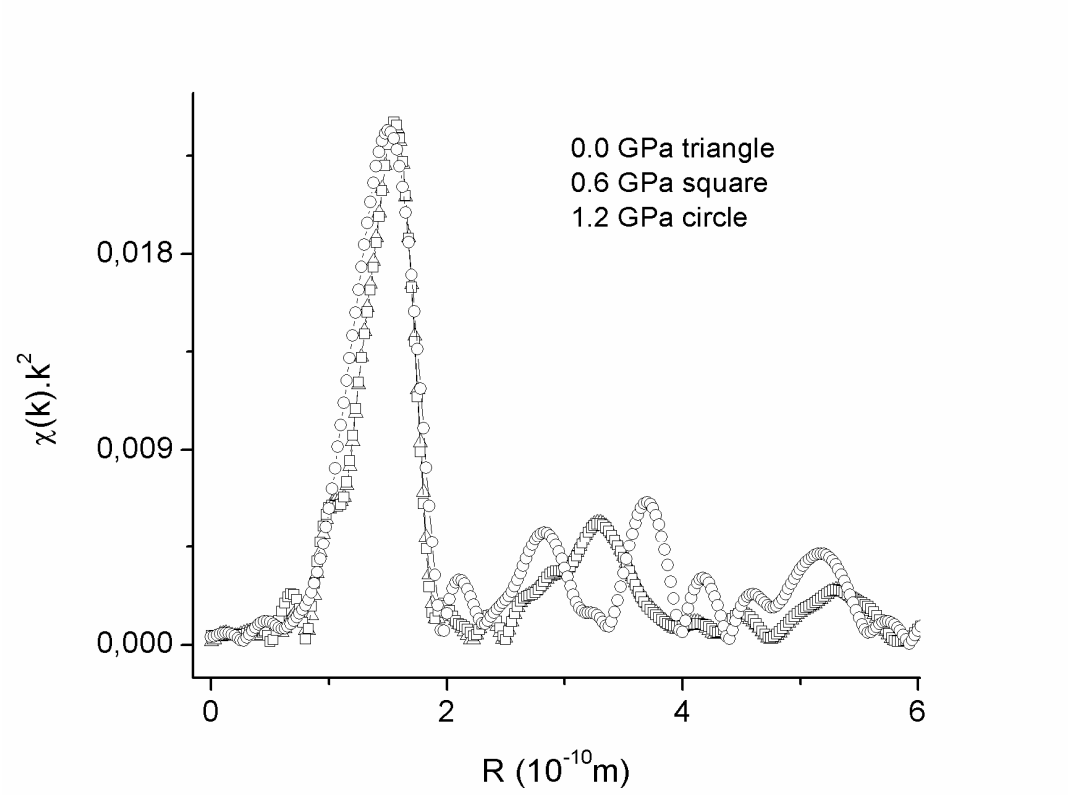

Figure 2 - The FFT of the EXAFS spectra for ambient pressure, 0.6 and 1.2 GPa.

The fitting results confirm that the lower symmetry of the rhenium site in the octahedron (out of the centre) was invariant up to 1.2 GPa. However, the EXAFS spectrum fitting using single and multiple scattering paths revealed that the 1.2 GPa configuration of ReO_6 octahedral in Ca_2MnReO_6 cannot be attributed to a single rotation angle for the ReO_6 rigid body among the octahedral. The ReO_6 octahedral configuration in Ca_2MnReO_6 at 1.2 GPa is similar to α-ReO_2 [30] and indicates a reduction of the Re2-Re1(i) distance.

3. CONCLUSIONS

The analysis of the EXAFS signal under external hydrostatic pressure indicated there is no change in the Re-O average distance in ReO_6 phase present in Ca_2MnReO_6. However, the

external pressure on the ReO_6 octahedral configuration in Ca_2MnReO_6 up to 1.2 GPa indicated a reduction of the Re2-Re1(i) distance and, as a consequence, of the plane undulation. This behaviour was attributed to a new ReO_6 octahedral configuration in Ca_2MnReO_6 without changing the ReO_6 distorted local symmetry (lower than D_{4h}). Other investigations are underway to clarify this question.

The new B_4C anvil cell with a Cu–Be body built for this study showed good performance for synchrotron radiation absorption studies at pressures up to 1.2 GPa, exhibiting reproducibility, simplicity of operation and low construction costs. For X-ray diffraction experiments it will be necessary to improve the portion of the diffraction pattern accessed in pressure-dependent measurements, taking into account the energy limitation (16 keV) of the LNLS.

ACKNOWLEDGMENTS

The authors would like to thank CNPq for financial support (projects 471536/04-0 and 54424/06-4) and the Brazilian Synchrotron Light Laboratory – LNLS for the use of its facilities (D04B-XAFS1, D06B-DXAS and D10B-XPD beamlines). We are grateful to Dr E. Granado for helpful discussions.

REFERENCES

1. J. Longo, R. Ward, *J. Am. Chem. Soc. 83* (1961) 2816.
2. A. W. Sleight, J. Longo, R. Ward, *Inor. Chem. 1*, (1962) 245.
3. J. M. D. Coey, M. Viret, S. von Molnar, *Adv. Phys*. 48 (1999) 167.
4. S. A. Wolf, D. D. Awschalom, R. A. Buhram, J. M. Daughton, S. von Molnár, M. L. Roukes, A. Y. Chtchelkanova, D. M. Treger, *Science* 294 (2001) 1488.
5. S. A. Wolf, A. Y. Chtchelkanova, D. M. Treger, *IBM J. Res. Dev.* 50, n. 1 (2006).
6. S. Parkin, X. Jiang, C. Kaiser, A. Panchula, K. Roche, M. Samant, *Proc. Of the IEEE* 91, n. 5 (2003).
7. P. Foldi, O. Kalman, M. G. Benedict, F. M. Peeters, *Nano Lett.* 8 (2008) 2556.
8. M. N. Leuenberg, M. E. Flatté, D. D. Awschalom, *Phys. Rev. Lett.* 94 (2005) 107401.
9. S. D. Sarma, J. Fabian, X. Hu, I. Zutic, *Solid State Comm.* 119, (2001) 207.
10. C.-Y. You, S. D. Bader, *J. Appl. Phys.* 87, (2000) 5215.
11. H. Dery, L. J. Sham, *Phys. Rev. Lett* 98, (2007) 046602.
12. A. Quesada, M. A. García, J. de La Venta, E. F. Pinel, J. M. Merino, A. Hernando, *Eur. Phys, J.* B 59 (2007) 457.
13. K.-I. Kobayashi, T. Kimura, H. Sawada, K. Terakura, Y. Tokura, *Nature* 395 (1998) 677.
14. Z. Zeng, I. D. Fawcett, M. Greenblatt, M. Croft, *Mater. Res. Bull.* 36 (2001) 705.
15. Z. Fang, K. Terakura, J. Kanamori, *Phys. Rev. B* 63, (2001) 180507(R).
16. G. Popov, M. V. Lobanov, E. V. Tsiper, M. Greenblatt, E. N. Caspi, A. Borissov, V. Kiryukhin, J. W. Lynn, *J. Phys. Cond. Matt.* 16, (2004) 135.
17. H. Kato, T. Okuda, Y. Okimoto, Y. Tomioka, K. Oikawa, T. Kamiyama, Y. Tokura, *Phys. Rev. B* 69 (2004) 184412.
18. J. B. Philipp, P. Majewski, L. Alff, A. Erb, R. Gross, T. Graf, M. S. Brant, J. Simon, T. Walther, W. Mader, D. Topwal, D. D, Sarma, *Phys. Rev B* 68, (2003) 144431.
19. M. W. Lufaso, P. W. Barnes, P. M. Woodward, *Acta Cryst. B* 62 (2006) 397.

20. D. Serrate, J. M. De Teresa, M. R. Ibarra, *J. Phys. Cond. Matt.* 19 (2007) 023201.
21. M.W. Lufaso, P.M. Woodward, *Acta Crystallogr., Sect. B: Struct. Sci.* 57 (2001) 725.
22. G. Popov, M. Greenblatt, M. Croft, *Phys. Rev. B* 67 (2003) 024406.
23. E. Granado, Q. Huang, J. W. Lynn, J. Gopalakrishnan, R. L. Grenee, K. Ramesha, *Phys. Rev. B* 66 (2002) 064409.
24. J. Herrero-Martín, G. Subías, J. Blasco, J. García, M. C. Sánchez, J. *Phys. Cond. Matt.* 17 (2005) 4963.
25. M. Sikora, Cz. Kapusta, M. Borowiec, C. J. Oates, V. Prochazka, D. Rybicki, D. Zajac, J. M. De Teresa, C. Marquina, M. R. Ibarra, *Appl. Phys. Lett.* 89 (2005) 062509.
26. Tolentino, H. C. N., Cezar, J. C.,Watanabe, N., Piamonteze, C., Souza-Neto, N. M., Tamura, E., Ramos, A. Y. & Neueschwander, R. (2005). *Phys. Scr.* T115, 977–979; AIP Conf. Proc. 705, 647–650.
27. Batlogg, B., Maines, R. G., Greenblatt, M. & DiGregorio, S. (1984). *Phys. Rev. B*, 29, 3762–3764.
28. Jørgensen, J.-E., Marshall, W. G., Smith, R. I., Staun Olsen, J. & Gerward, L. (2004). *J. Appl. Cryst.* 37, 857–861.
29. B. Houser and R. Ingalls, "X-ray Absorption Fine Structure Determination of Pressure Induced Bond Angle Changes in ReO(3)," Phys. Rev. B61, 6515 (2000).
30. Fabio Furlan Ferreira, Hamilton P. S. Correa, Marcos T. D. Orlando, Jose L.Passamai, Cintia G. P. Orlando, Isabela P. Cavalcante, Flavio Garcia, Edilson Tamura, Luis G. Martinez, Jesualdo L. Rossi and Francisco C. L. de Melo, *J. Synchrotron Rad.* (2009). 16, 48–56